

Measurements of Stark-broadened Balmer α and γ lines of He II in dense plasmas

J. Musielok,* F. Böttcher, H. R. Griem,† and H. -J. Kunze

Institut für Experimentalphysik V. Ruhr-Universität Bochum, Postfach 102148, D-4630 Bochum 1, West Germany

(Received 9 June 1987)

We have measured profiles of optically thin Balmer α and γ lines of He II at 164 and 108.5 nm in a homogeneous hydrogen plasma using a microchannel-plate detector. The electron density of the plasma is between 5×10^{23} and $8 \times 10^{23} \text{ m}^{-3}$ at temperatures of about 10 eV. The measured line profiles and full-widths at half maximum are compared with various calculations and measurements. We find agreement for the Balmer α line within the experimental errors of approximately 25%. The Balmer γ line is less broadened than expected from the calculation of Kepple, as found in two earlier experiments.

I. INTRODUCTION

Experimental studies of line shapes for hydrogenic ion emitters are of general interest in connection, e.g., with diagnostic measurements on high-temperature and high-density plasmas or with accurate wavelength measurements. As ionized helium is the prototype system for one-electron ions, many theoretical¹⁻³ and experimental⁴⁻¹² studies have concentrated on the broadening of ionized helium lines. Also the rather small shifts of the lines and their asymmetries have been the subject of numerous experimental^{13,14} as well as theoretical papers.^{15,16} In spite of growing interest and much effort the agreement between theoretical and experimental results is not satisfactory.

On the other hand, the broadening of the Paschen α line of He II at 468.6 nm is routinely used to determine the electron density in plasmas. This is mainly due to the fact that this line is in a very convenient spectral range for spectroscopic measurements and that several studies have been performed on the broadening of this line with independent-electron density measurements.

For the Balmer lines of He II in the vacuum-uv (vuv) spectral range, however, the situation is not satisfactory. There the discrepancies between different theoretical approaches are rather large and only a few measurements are available. Some of these broadening measurements are disturbed considerably by self-absorption effects in the line core (especially in the case of the Balmer α line^{5,6,14}). Moreover, almost all measurements were performed scanning the profile from discharge to discharge, relying on the reproducibility of the plasmas. The measurements of Pittman and Fleurier¹⁴ were performed applying a multichannel detector but their broadening results are strongly affected by self-absorption in the line core.

In this work we avoid both difficulties: Using the gas-liner pinch as an emission source we avoid self-absorption effects in the plasma, and applying a combination of a microchannel plate (MCP) with an optical multichannel analyzer (OMA), we are able to obtain the entire line profile during one shot and with good time resolution.

II. EXPERIMENT

The experimental arrangement is shown schematically in Fig. 1. The plasma was produced in the gas-liner pinch as described in detail in Refs. 17-19. Hydrogen was applied as a driver gas. Because the Balmer lines of He II are very intense, the introduction of very small amounts of He ($\approx 1\%$) in the center of the discharge was sufficient.

The $\frac{1}{4}$ -m monochromator was used for monitoring the continuum radiation of the plasma at 544 nm. Near this wavelength the continuum emitted by the gas-liner pinch

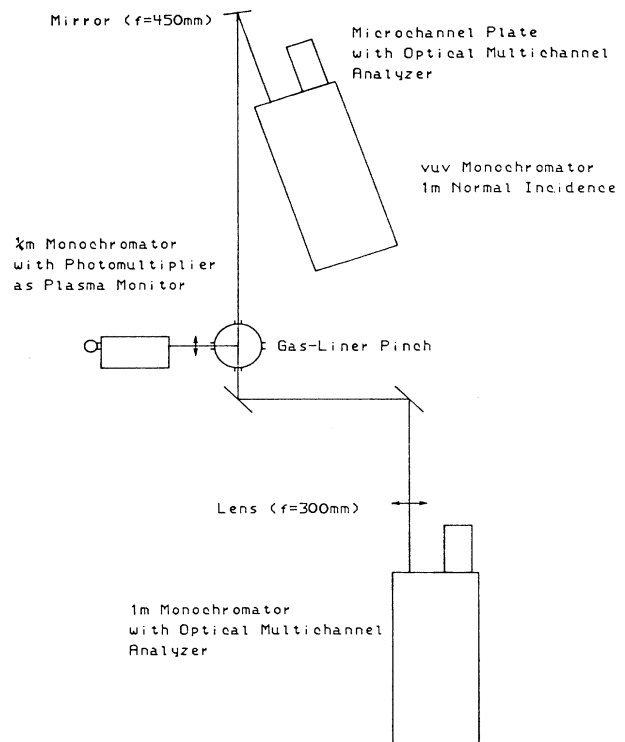


FIG. 1. Experimental set-up.

working with hydrogen as driver gas is not influenced by hydrogen emission lines nor by lines arising from the test gas or other impurities. The continuum intensity clearly indicates the moment of maximum compression of the plasma. The continuum intensity was monitored using a storage oscilloscope to check the reproducibility of the discharge. Simultaneously the pulse gating of the detection systems was monitored. In this manner the timing of the radiation detection with respect to the plasma evolution was obtained.

The 1-m grating monochromator (entrance slit 25 μm) equipped with an optical multichannel analyzer (OMA) was applied for diagnostic measurements (broadening of the Paschen α line of He II at 468.6 nm). The time resolution was achieved by gating the OMA during a time interval of 20 ns. The reciprocal dispersion of this detection system is 0.0205 nm/channel. The apparatus profile was obtained using a Zn spectral lamp as an emission source. The profile of the Zn I line at 472.2 nm could be approximated with a Voigt profile of a Lorentzian full width at half maximum (FWHM) of 0.09 nm and a Gaussian FWHM of 0.02 nm. For the measurements in the vuv a 1-m normal incidence monochromator with a concave grating of 1200 lines/mm was available. A gated multichannel plate of chevron type was placed in the exit slit plane of the monochromator. The image of the spectrum which appears on the phosphor screen of the MCP is recorded with a second OMA system. This detection system allows us to record spectra with good spectral resolution (reciprocal dispersion 0.01 nm/channel, apparatus profile of FWHM of 0.09 nm, both in second order) as well as with sufficient time resolution (~ 30 ns). Detailed data concerning the vuv detection system may be found in our previous work.²⁰

III. DETERMINATION OF THE PLASMA PARAMETERS

The most important quantity for the line-broadening study is the electron density (ion density). Since we use hydrogen as the driver gas and only a very small amount of helium, we can assume that the electron density and the ion density are the same. We can also assume that only electrons and hydrogen ions (protons) are playing an important role in the formation of He II spectral line profiles. Because the emission of He II occurs from a volume of rather constant electron density¹² no Abel inversion is required for the determination of the local line profile.

The electron density N_e was obtained from the measured width of the P_α line of He II at 468.6 nm. The empirical relation proposed by Pittman and Fleurier²¹ was applied:

$$N_e / \text{m}^{-3} = 3.31(\Delta\lambda_{1/2})^{1.21} \times 10^{23}, \quad (1)$$

where $\Delta\lambda_{1/2}$ is the full width at half maximum of the Stark-broadened P_α line in nanometers. On the basis of several recorded P_α line profiles the electron density values of $7.7 \times 10^{23} \text{ m}^{-3}$ for the maximum compression (Expt. I) and $4.7 \times 10^{23} \text{ m}^{-3}$ for 120 ns after maximum

compression (Expt. II) were found. For the evaluation of the Stark FWHM the contributions from the apparatus and Doppler broadening were taken into account. At nearly the same plasma conditions, independent-electron density measurements based on the absolute value of the continuum radiation have recently

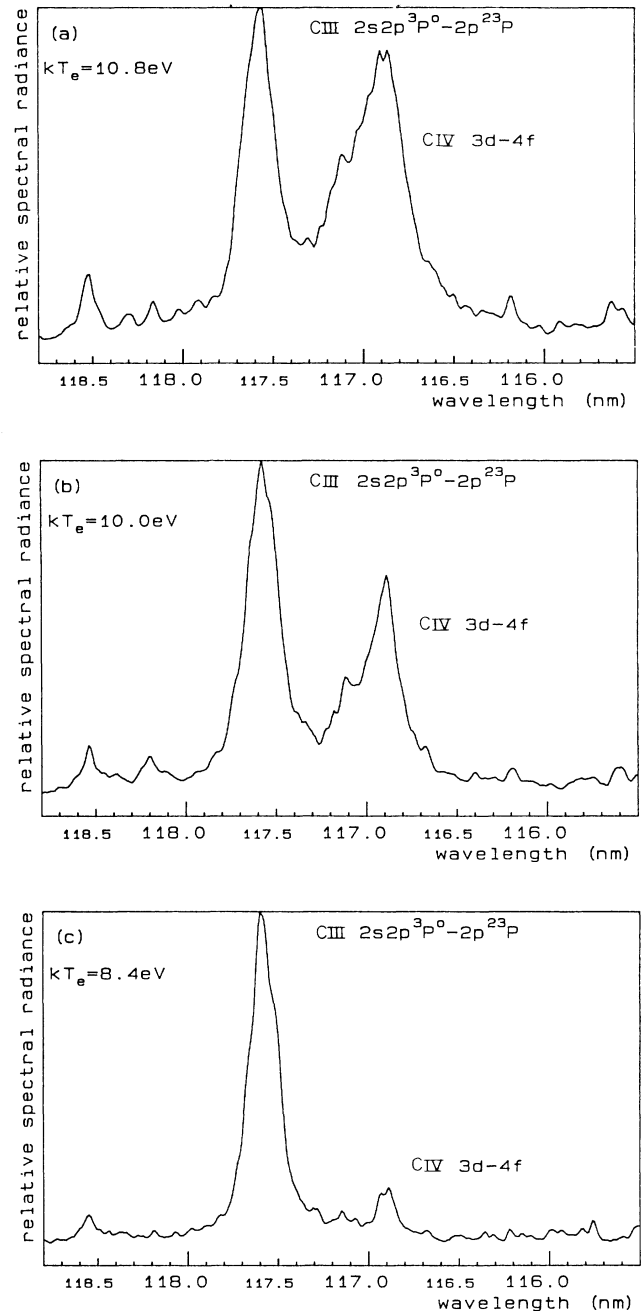


FIG. 2. vuv single-shot spectra from the wavelength range 115.5–119 nm recorded at different times: (a) maximum compression, (b) 100 ns, and (c) 270 ns after maximum compression. The temperatures are evaluated from the intensity ratio of CIV to CIII lines.

been performed by Ackermann *et al.*¹² confirming the validity of formula (1) even at our relatively high electron temperatures. The uncertainty of the electron density determination arising from the reproducibility of the discharge does not exceed 15%. The accuracy of formula (1) itself is estimated to about 10%, leading to an experimental uncertainty of at most 25%.

To obtain the temperature of the plasma, methane was used as a test gas. As pointed out in Ref. 19, the change of the test gas does not influence the plasma parameters (N_e and T) as long as the amount of test gas is small compared with the amount of the driver gas. The temperature was derived from the line intensity ratio of two lines in subsequent ionization stages C III and C IV. The vacuum-uv lines at 116.9 nm of C IV and 117.6 nm of C III were chosen. These lines are so close in wavelength that intensity measurements in relative units are sufficient for temperature determination. The temperature dependence of this line intensity ratio was calculated on the basis of theoretical results for the intensity ratio of uv lines at 253.0 and 229.7 nm.²² The transition probabilities (A_{ki}) for the uv and vuv transitions were taken from Cheng *et al.*²³ (C III lines) and the values of C IV are based on the Coulomb approximation.²⁴ Because the A_{ki} value for the C III line 229.7 nm obtained by Cheng *et al.* differs from the value previously used²², an additional correction was necessary. According to Ref. 22 this method of temperature evaluation can be applied for electron densities not exceeding 10^{23} m^{-3} . However, theoretical errors caused by deviations from the model used in Ref. 22 on the approach to complete local thermodynamic equilibrium are not likely to exceed ~ 1 eV, because the temperature dependence of the line ratio is very strong.

In Fig. 2, three single-shot spectra in the wavelength range 115.5–119 nm recorded at different times are presented. This figure clearly indicates the time evolution of the plasma temperature.

The mean temperature values obtained from several spectra are as follows: for Expt. I, 10.7 eV and for Expt. II, 9.8 eV. Additional temperature measurements based on a C IV–C III line intensity ratio in the visible range of the spectrum near 466 nm were also performed. We found good agreement between the two measurements. Recently Böttcher *et al.*²⁵ have evaluated the temperature of the plasma produced in the same device by means of absolute measurements of the blackbody-limited line intensity for the $2s$ - $2p$ transition of C IV. The temperature obtained in this manner is only slightly smaller than obtained in this work. This discrepancy mainly results from different amounts of test gas used in these two experiments.

IV. RESULTS AND DISCUSSION

The He II Balmer α transition between the levels 2 and 3 consists of seven fine-structure components. The wavelength separation between the two strongest components is 0.014 nm. The level splitting due to linear (strong field) Stark effect for a given electric field is proportional to the principal quantum number n and to the

difference between the two parabolic quantum numbers $n_1 - n_2$. In order to compare the fine-structure splitting with the Stark splitting, the wavelengths of the individual Stark components for perturber distances typical for our plasma densities were computed. In the calculations the quadrupole effects were also taken into account.²⁶ The fine-structure splitting and the Stark splitting show opposite dependence on the principal quantum number n . The most critical level for fine structure is therefore the level $n=2$. The fine-structure splitting of this level is 6 cm^{-1} . The Stark splitting typical for our plasma conditions is 40 cm^{-1} and 29 cm^{-1} for Expt. I and Expt. II, respectively. Thus the influence of the fine structure is small in comparison with the action of the linear Stark effect. The broadening of the transition 2-3 ($\lambda=164.0$ nm) due to thermal Doppler effect leads to a FWHM of 0.02 nm, while the FWHM arising from Stark effect amounts according to Kepple¹ to 0.1 and 0.06 nm for Expt. I and Expt. II, respectively.

To obtain spectral resolution sufficient for reliable line-broadening measurements we have recorded the Balmer α line (164.0 nm) in the second order of the spectrum. The apparatus profile of our vuv detection system was obtained from the profile of the Ni transition $^2P^o - ^2D$ at 141.2 nm emitted from an NBS-miniarc²⁷ running at a current of 15 A. The broadening of this line due to the Stark and Doppler effects can be neglected (low density and low temperature). The apparatus profile obtained in this manner was convolved with the Doppler profile for the 164.0-nm line. The FWHM of the resulting profile is 0.091 nm. In Fig. 3(b) this profile is compared with the Balmer α profile measured in Expt. I. In Fig. 3(a) the measured profile is compared with the profile calculated according to Refs. 1 and 28 for our plasma conditions ($N_e = 7.7 \times 10^{-23} \text{ m}^{-3}$; $kT_e = 10.7$ eV). The measured line shapes shown in Fig. 4 are superpositions of eight and twelve individual measurements for Expt. I and Expt. II, respectively. The individual line shapes are somewhat more noisy, but the important parameters (e.g., the fractional widths) of each line profile are very close to those of the mean line profiles. In order to obtain the background continuum radiation for this line, the radiation of the pure hydrogen plasma was recorded. This reveals that the continuum intensity remains nearly constant in the spectral range which can be simultaneously detected by the OMA array (7 nm in the second order). These tests show also that the wavelength dependence of the efficiency of our detection system does not change, at least not in the wavelength range important for the line-broadening study.

As shown in Ref. 25, with increasing amounts of test gas the line intensity increases, but at a certain concentration the studied line may become optically thick, without showing any strong line reversal effects. To avoid self absorption effects for our Balmer α measurements, only very small amounts of helium were introduced into the discharge volume. With increasing amounts of helium we could still observe an increasing intensity in the line center of the Balmer α line.

To check how far the line center intensity is from the blackbody limit, we compared the intensity of optically

thick C IV $2s-2p$ radiation at 155 nm with the Balmer α line core intensity. Assuming that the efficiency of our detection system does not change considerably in the spectral range 155–164 nm, we found an intensity ratio of 210. The optically thick conditions for the C IV resonance line were achieved by increasing the amount of methane by a factor of 10 compared with the usually applied amounts of test gas.²⁰

The theoretical profiles corresponding to our plasma conditions were computed on the basis of the tables published in Ref. 28. The computed profiles were numerically convolved with the corresponding apparatus and Doppler profiles. Figure 4 shows the computed theoretical profiles and the measured profiles for Expt. I and Expt. II. The profiles are peak normalized, because area normalization would lead to somewhat ambiguous results, owing to the background radiation. Our spectral resolution was too poor for accurate wavelength measurements (line-shift studies), thus the maxima of both profiles—theoretical and experimental—presented in Fig. 4 were set at the same wavelength.

The comparisons show a rather good agreement, especially for Expt. II. The systematic discrepancy in the

line core observed mainly in Expt. I may arise partly from the difficulties in the determination of the true underlying continuum radiation. The asymmetry observed in the line core, however, cannot be explained in this way.

In calculations performed by Kepple¹ [the reduced profiles $S(\alpha)$ are published in Ref. 28], the influence of the radiator and perturber motion (ion-dynamic effect) was neglected. It affects mainly the shape near the line center and leads to a wider line profile.³ The maximum of the Balmer α line is determined mainly by the position of the central Stark component. Due to the ion quadrupole effects, the central component is blue shifted, whereas electron collisions cause even larger red shifts.¹⁶ In Kepple's calculations these effects were also neglected. In our profile comparison in Fig. 4 such shifts are obviously cancelled by setting both maxima at the same wavelength. The discrepancies arising mainly at higher plasma density (different intensity gradients in the line core) could perhaps be interpreted as a result of quadrupole interactions between the He II emitters and the perturbing protons. Theoretically, the three strongest Balmer α Stark components are blue shifted, the shift of the central component, however, is two times larger than that of the neighboring components. This would lead to an enhanced blue line core, in contrast to what is observed in our experiment. Consideration of intensity corrections for the various components (see Ref. 16) do not change this conclusion, but suggest that the asymmetry from quadrupole effects is also much too small quantitatively. Asymmetries from differences in electron-produced shifts of the various components should be negligible as well.

As mentioned above, the energy splitting of the levels under consideration due to Stark effect dominates over the fine-structure splitting. In order to check how the neglected fine structure may influence the theoretical profile, the following calculations have been performed. The superposition of the seven fine-structure components weighted according to their intensities was calculated, assuming that each component is Doppler and Stark broadened. The intensities of the fine-structure components were taken from Ref. 29. This asymmetric profile was convolved with the corresponding apparatus profile. The resulting profile does not show any significant asymmetry. The FWHM is only 3% wider than that obtained without fine-structure splitting.

Figure 5(a) shows the spectrum in the wavelength range from 107 to 112 nm recorded at maximum compression. The steep decrease of the signal below 107 nm is caused by the reduced efficiency near the edge of the OMA detector. The He II Balmer γ line is disturbed by the far wings of the O VI $2s-2p$ resonance transition at 103.4 nm. Applying a fitting procedure which takes into account the influence of the O VI line wing as well as the continuum radiation, the "true" Balmer γ line shape is obtained. Figure 5(b) shows the experimental profile and theoretical profiles after Ref. 28. The theoretical profiles include the apparatus and Doppler broadening.

The measurements in the case of the Balmer γ profile are less accurate than those of the Balmer α profile.

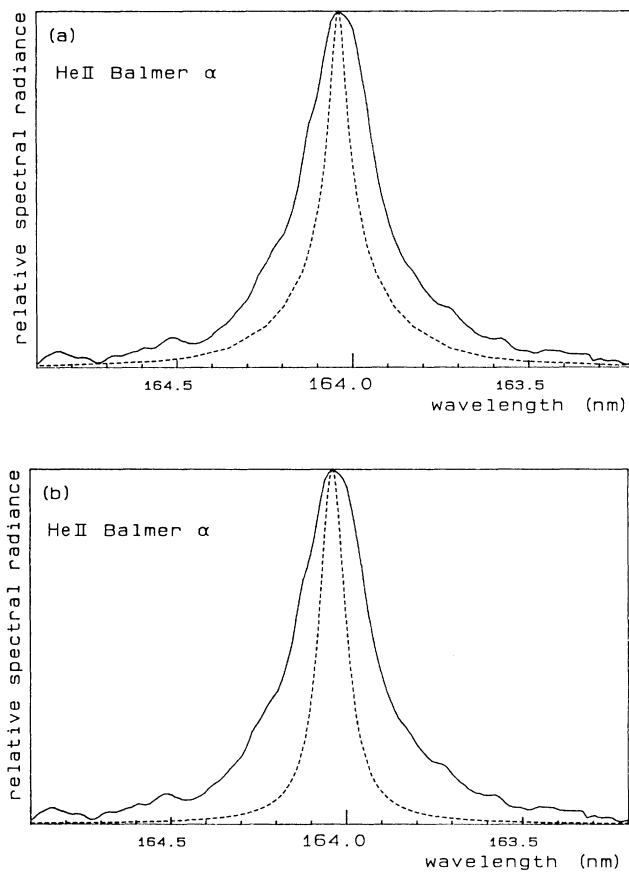


FIG. 3. Comparison of the measured He II Balmer- α profile (solid curves): (a) with the corresponding Stark profile (Ref. 28) and (b) with the resulting profile from the convolution of apparatus and Doppler profiles.

However, at the nominal densities the discrepancies between theoretical and experimental profiles are beyond the experimental uncertainty. The theory predicts 30% larger FWHM than obtained in our experiment. All measurements performed to date had indicated this discrepancy.^{5,7}

In order to compare our results with other measurements and theoretical results, the fractional widths in reduced wavelength units $\alpha_{1/2}$ were calculated. In Fig. 6 the $\alpha_{1/2}$ values obtained in this work for the Balmer- α and - γ lines are compared with other theoretical and experimental results. Direct comparison is only possible with results of Kepple¹ (published also in Ref. 28). The $\alpha_{1/2}$ values for our plasma conditions can be found by interpolation in the tables of Kepple.¹ Other theoretical results are obtained only for certain plasma conditions (the corresponding temperature values are given in the caption of Fig. 6).

An alternative interpretation of the line profile measurements is to assume that the true electron density is

near the lower limit permitted by the experimental error in this quantity, say, at $5.8 \times 10^{23} \text{ m}^{-3}$ and $3.5 \times 10^{23} \text{ m}^{-3}$, respectively, for Expt. I and Expt. II. As shown in Fig. 5(b), a much better fit with Kepple's He II Balmer- γ profile calculation is now obtained, with residual deviations of $\sim 10\%$; of course, Kepple's calculated He II Balmer- α profiles, corrected for fine-structure, Doppler, and instrumental broadening, turn out to be too narrow by about 15% or 10% for the two experimental conditions [see Figs. 4(c) and 4(d)].

This deficiency of the calculated profiles can be explained in terms of ion-dynamical effects, which give additional broadening typically of the order of the ion plasma frequency³⁰ or v_i/r_0 (the ratio of ion thermal speeds and mean separations) and may be modeled by convolution with a Gaussian.³¹ (The latter paper overestimates the actual effects, because it uses an expansion which is not appropriate if the corrections to the quasistatic ion-broadening calculations are found to be large.) Profiles calculated using such additional contribution to the

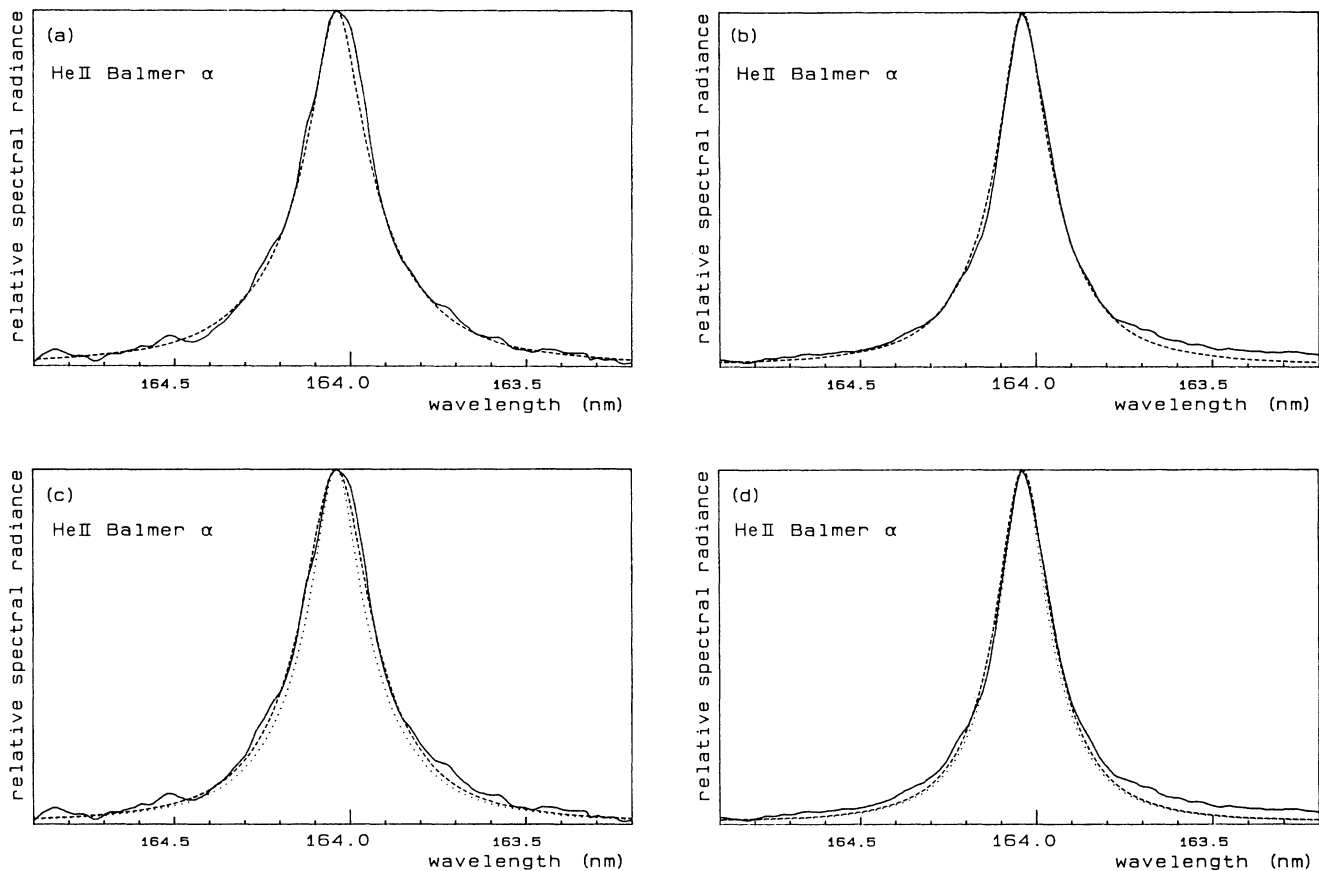


FIG. 4. Comparison of experimental (solid) and theoretical (dashed and dotted) line profiles for He II Balmer- α . The theoretical Stark profiles are calculated from data given in Ref. 28 at the plasma parameters given below and convolved with the corresponding apparatus and Doppler profiles. (a) $N_e = 7.7 \times 10^{23} \text{ m}^{-3}$, $kT_e = 10.7 \text{ eV}$; (b) $N_e = 4.7 \times 10^{23} \text{ m}^{-3}$, $kT_e = 9.8 \text{ eV}$. (c) $N_e = 5.8 \times 10^{23} \text{ m}^{-3}$, $kT_e = 10.8 \text{ eV}$ (dotted profile): the dashed profile is additionally convolved with a Doppler profile with a FWHM of 0.08 nm corresponding to five times the ion plasma frequency. (d) $N_e = 3.5 \times 10^{23} \text{ m}^{-3}$, $kT_e = 9.8 \text{ eV}$ (dotted profile). The dashed profile is additionally convolved with a Doppler profile with a FWHM of 0.05 nm corresponding to four times the ion plasma frequency.

Gaussian width are also shown in Figs. 4(c) and 4(d). They do agree within the experimental error. Corresponding corrections for the He II Balmer- γ line are negligible.

We must point out here that profiles calculated according to Greene³ would probably have been narrower by less than 20% after the various corrections for other broadening mechanisms. Such profiles are not available in the literature, but would evidently agree best with the measured profiles at electron densities about halfway between the nominal densities in our experiments and those near the lower limit of our electron density measurements.

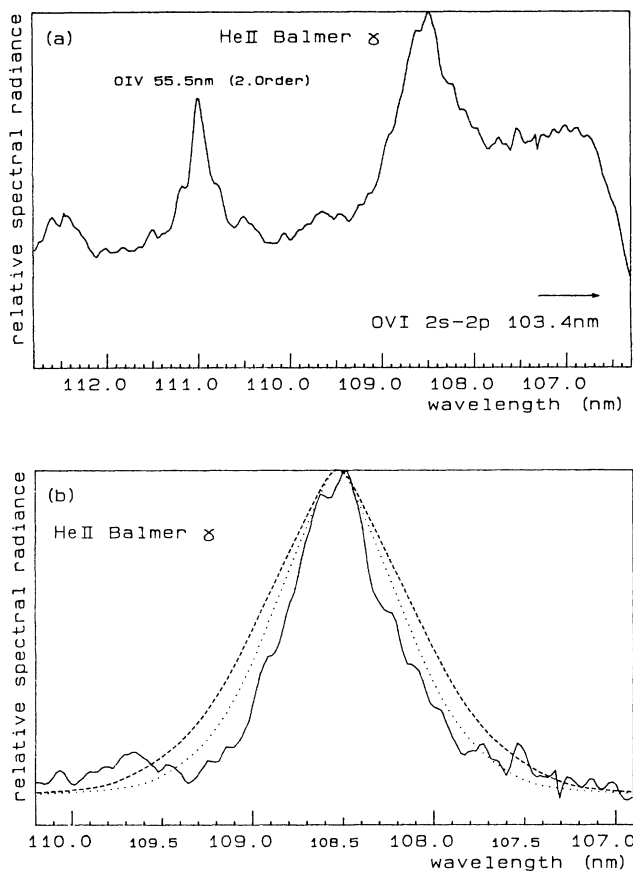


FIG. 5. (a) Measured spectrum in the wavelength range from 107 to 112 nm. The steep decrease of the signal at wavelengths below 107 nm is due to decreasing efficiency on the edge of the detector system. The He II Balmer- γ line is disturbed by the wings of the O VI 2s-2p resonance transition. (b) Comparison between measured (solid) and theoretical (dashed and dotted) He II Balmer- γ line profiles. The theoretical profiles are calculated from data given in Ref. 28 and convolved with the corresponding apparatus and Doppler profiles. The measured profile was obtained from the spectrum shown in (a) by subtracting the continuum and the far wing of the O VI resonance line. Dashed profile: $N_e = 7.7 \times 10^{23} \text{ m}^{-3}$, $kT_e = 10.7 \text{ eV}$; dotted profile: $N_e = 5.8 \times 10^{23} \text{ m}^{-3}$, $kT_e = 10.7 \text{ eV}$.

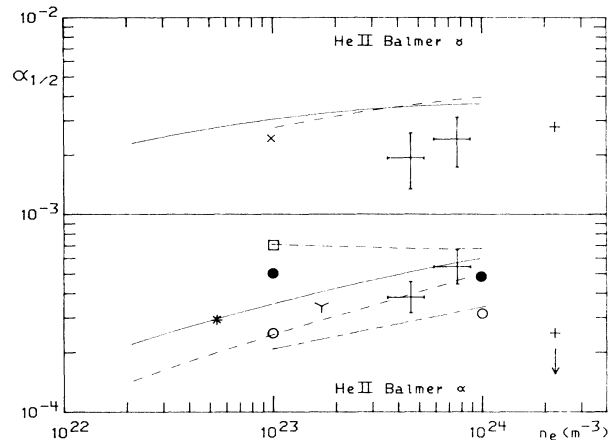


FIG. 6. Experimental values and theoretical values of the fractional intensity width $\alpha_{1/2}$ (in cgs units) of He II Balmer α and Balmer γ are shown as a function of electron density. An additional parameter is the electron temperature given below in brackets. Theoretical data: —, Kepple (Ref. 1) (1971) (3.45 eV); ---, Kepple (Ref. 1) (1971) (13.8 eV); - - - -, Oza (Ref. 35) (1987), static (9 eV); - · - · - ·, Oza (Ref. 35) (1987), dynamic (9 eV); □, Lee (Ref. 2) (1979) (3.5 eV); ○, Greene (Ref. 3) (1982), static (3.6 eV at $N_e = 10^{23} \text{ m}^{-3}$ and 8.8 eV at $N_e = 10^{24} \text{ m}^{-3}$); ●, Greene (Ref. 3) (1982), dynamic (as in the static case). Experimental data: +, Hessberg and Böttcher (Ref. 5) (1967) (4.3 eV); ×, Eberhagen and Wunderlich (Ref. 7) (1970) (20 eV); Y, Jones *et al.* (Ref. 4) (1971) (4–5 eV); *, Piel and Slupek (Ref. 11) (1984) (3.8 eV); —|—, our measurements.

As discussed by Greene,³ the reason for his narrower Stark profiles, before ion-dynamical corrections, lies in a different treatment of the upper-lower state interference term in the electron impact broadening. This term has been subject to some theoretical controversy^{32,33} and its treatment can probably not really be separated from that of low frequency Stark effects, i.e., from ion dynamics. Calculations including the full interference effect and ion dynamics, as well as experiments with more accurate density diagnostics, are therefore needed to settle the remaining differences, say, at the $\pm 10\%$ level.

V. CONCLUSION

The measured line profiles of the He II Balmer- α line are in agreement with the only available profile calculations for our plasma conditions by Kepple.¹ From a recent calculation of Oza *et al.*³⁴ we estimate the additional ion-dynamical effects on the full width at half maximum of the line profile to about 10–20% of our measured FWHM, which is just within our experimental error.³⁵

Since these ion-dynamical effects are relatively small at higher densities, more accurate density diagnostics and line profile calculations at various plasma conditions are necessary to arrive at final conclusions regarding

their precise magnitude. The situation is quite different for the He II Balmer- γ line. Here our measured profiles are narrower than expected from the calculations of Kepple, and this deviation cannot be explained by ion-dynamical effects. It is also unlikely that the interference term in the electron broadening is responsible for the difference in the profiles.

ACKNOWLEDGMENTS

This work was supported by the Sonderforschungsbereich 162 (Plasmaphysik Bochum/Jülich). One of us (H.R.G.) was supported by the A.v. Humboldt Foundation. The authors are grateful to Dr. D. H. Oza for making his calculation of the Balmer- α line available.

*Permanent address: Institute of Physics, Pedagogical University Opole, 45-052 Opole, Poland.

†Permanent address: Laboratory for Plasma and Fusion Energy Studies, University of Maryland, College Park, Maryland 20742.

- ¹P. C. Kepple, Phys. Rev. A **6**, 1 (1972); University of Maryland Report No. 72-018, 1971.
- ²R. W. Lee, J. Phys. B **12**, 1129 (1979).
- ³R. L. Greene, Phys. Rev. A **14**, 1447 (1976); J. Phys. B **15**, 1831 (1982).
- ⁴L. A. Jones, J. R. Greig, T. Oda, and H. R. Griem, Phys. Rev. A **4**, 833 (1971).
- ⁵J. Hessberg and W. Böttcher, Z. Naturforsch. Teil A **22**, 316 (1967).
- ⁶C. C. Smith and D. D. Burgess, J. Phys. B **11**, 2087 (1978).
- ⁷A. Eberhagen and R. Wunderlich, Z. Phys. **232**, 1 (1970).
- ⁸Y. Arata, S. Miyake and H. Matsuoka, J. Quant. Spectrosc. Radiat. Transfer **32**, 343 (1984).
- ⁹M. E. Bacon, A. J. Barnard, and F. L. Curzon, J. Quant. Spectrosc. Radiat. Transfer **18**, 399 (1977).
- ¹⁰T. Oda and S. Kiriya, J. Phys. Soc. Jpn. **49**, 385 (1980).
- ¹¹A. Piel and J. Slupek, Z. Naturforsch. Teil A **39**, 1041 (1984).
- ¹²U. Ackermann, K. H. Finken, and J. Musielok, Phys. Rev. A **31**, 2597 (1985).
- ¹³K. Murakawa, J. Phys. Soc. Jpn. **52**, 1969 (1983).
- ¹⁴T. L. Pittman and C. Fleurier, Phys. Rev. A **33**, 1291 (1986).
- ¹⁵T. L. Pittman, P. Voigt, and D. E. Kelleher, Phys. Rev. Lett. **45**, 723 (1980).
- ¹⁶H. R. Griem, Phys. Rev. A **27**, 2566 (1983).
- ¹⁷K. H. Finken and U. Ackermann, Phys. Lett. **85A**, 279 (1981).
- ¹⁸K. H. Finken and U. Ackermann, J. Phys. D **15**, 615 (1982).
- ¹⁹K. H. Finken and U. Ackermann, J. Phys. D **16**, 773 (1983).
- ²⁰F. Böttcher, J. Musielok, and H.-J. Kunze, Phys. Rev. A **36**, 2265 (1987).
- ²¹T. L. Pittman and C. Fleurier, in *Spectral Line Shapes*, edited by K. Burnett (deGruyter, New York, 1983), Vol. II.
- ²²H. R. Griem, *Plasma Spectroscopy* (McGraw-Hill, New York, 1964).
- ²³K. T. Cheng, Y.-K. Kim, and J. P. Desclaux, At. Data Nucl. Data Tables **24**, 111 (1979).
- ²⁴D. R. Bates and A. Damgaard, Philos. Trans. R. Soc. London, Ser. A **242**, 101 (1949).
- ²⁵F. Böttcher, U. Ackermann, and H.-J. Kunze, Appl. Opt. **25**, 3307 (1986).
- ²⁶G. V. Sholin, Opt. Spectrosc. **26**, 275 (1969).
- ²⁷J. M. Bridges and W. R. Ott, Appl. Opt. **16**, 367 (1977).
- ²⁸H. R. Griem, *Spectral Line Broadening by Plasmas* (Academic, New York, 1974).
- ²⁹H. A. Bethe and E. E. Salpeter, *Quantum Mechanics of One- and Two-Electron Atoms* (Springer, Berlin, 1957).
- ³⁰R. Stamm, B. Talin, E. L. Pollock, and C. A. Iglesias, Phys. Rev. A **34**, 4144 (1986).
- ³¹R. Cauble and H. R. Griem, Phys. Rev. A **27**, 3187 (1983).
- ³²D. Voslamber, Phys. Rev. A **14**, 1903 (1976).
- ³³H. R. Griem and J. D. Hey, Phys. Rev. A **14**, 1906 (1976).
- ³⁴D. H. Oza, R. L. Greene, and D. E. Kelleher, Phys. Rev. A (to be published).
- ³⁵D. H. Oza (private communication). After submission of this paper Oza has kindly made available computations of the Stark-broadened profile of the He II Balmer- α transition for our plasma conditions, i.e., for our electron density, temperature, and for protons as the perturbing ions. The calculation includes dynamical contributions of perturbing ions to the line profile. After convolution with the Doppler and apparatus profiles we find agreement with the corresponding result based on the Kepple-Griem calculation, especially in the half-maximum intensity range of the profile. For wavelengths beyond the half-width, the Kepple-Griem results fit better the measured profile whereas within the half-width Oza's calculation is closer to our measurement. The reduced wavelength values $\alpha_{1/2}$ of Oza in the static approximation as well as when including ion-dynamical effects have been added to Fig. 6.